0022-1554/80/1111-0809$02.25
The Journal of Histochemistry and Cytochemistry
Vol. 28, No. 11, pp. 1198–1206, 1980
Printed in U.S.A.
Copyright © 1980 by The Histochemical Society, Inc.

Preparation and Characterization of a New Molecular Cytochemical Probe:

5-Iodoacetamidofluorescein-labeled Actin[1]

YU-LI WANG and D. LANSING TAYLOR

Cell and Developmental Biology, The Biological Laboratories, Harvard University, Cambridge, Massachusetts 02138

Received for publication February 4, 1980 and in revised form May 2, 1980 (OA 80-116)

The new technique of molecular cytochemistry (Taylor DL, Wang YL (1978): Proc Natl Acad Sci USA 75:857) requires the use of functional fluorescent analogs of cellular components with optimal fluorescence characteristics. An analog of actin suitable for this technique is prepared by reacting purified rabbit striated muscle actin with 5-iodoacetamidofluorescein (5-IAF). The conjugate is purified by DEAE-cellulose ion exchange chromatography and cycles of polymerization–depolymerization, yielding a relatively homogeneous product with the fluorescein group covalently attached to cysteine 373. The fluorescently labeled actin maintains normal polymerizability and activates heavy meromyosin Mg^{2+} adenosine triphosphatase to the same extent as unlabeled actin. Furthermore, fluorescent paracrystals are readily detectable in fluorescence microscope upon adding excess Mg^{2+} or Ni^{2+} ions. Spectrofluorimetric studies of the bound fluorescein indicate that the peak excitation and emission wavelengths, the shapes of the spectra, and the peak fluorescence intensities are somewhat sensitive to polymerization and heavy meromyosin binding. Possible causes of these spectral changes are analyzed and future applications of this fluorescently labeled actin in vitro as well as in vivo are discussed.

KEY WORDS: Molecular cytochemistry; Fluorescently labeled actin; 5-Iodoacetamidofluorescein; Fluorescence spectroscopy.

Introduction

The self-assembly of actin and the interactions between actin and other muscle proteins have been studied intensively during the past two decades (for a review, see ref. 22). Recent investigations on nonmuscle cells have revealed important new roles of actin in many nonmuscle processes such as ameboid movement, cytokinesis, and membrane receptor redistribution (for reviews, see refs. 13, 24, and 30). Many proteins have been shown to interact with actin, including various gelatin factors (for reviews, see refs. 13 and 30), profilin (1), nonmuscle actinins (9), spectrin (18), DNase I (14), and even some glycolytic enzymes (13), making actin one of the most versatile proteins in eukaryotic cells.

Fluorescence spectroscopy has been a powerful tool for studying protein–protein interactions. Fluorescent probes such as *N*-(3-pyrene) maleimide (11), *N*-iodoacetyl-*N'*-(5-sulfo-1-naphthyl)-ethylenediamine (10, 25, 29), *N*-(*p*-(2-benzimidazolyl)-phenyl) maleimide (26), dansyl cystine (2), and dansyl aziridine (15, 25), have been coupled to actin. Using various fluorescence spectroscopic techniques, much information has been obtained regarding the biochemical activities of actin in vitro. In an attempt to extend the applicability of fluorescence techniques to living cells, we have recently introduced the technique of in vivo molecular cytochemistry, using functional fluorescent analogs of cellular components (31). The procedure involves purifying the cellular component under study, labeling with appropriate fluorophores, testing the conjugates for functional activities in vitro, and incorporating the conjugates into living cells using microinjection techniques. Subsequent recording of fluorescence images from injected cells allows direct determinations of the distribution of the conjugate and opens the possibility of extending spectroscopic methods to living cells.

To be suitable for applications in living cells, the fluorescent analog must meet at least four criteria: 1) The fluorophore should be excited by a relatively long wavelength of light, so that radiation damage to living cells and interference from autofluorescence can be minimized; 2) The fluorophore should emit intense fluorescence (by having a high extinction coefficient and/or a high quantum yield), in order to maximize the signal level from single cells; 3) The bond between the fluorophore and the labeled component must be covalent and

[1]This research was supported by the Institute of Arthritis, Metabolism and Digestive Disease Research Grant AM 18111, National Science Foundation NSF Grant PCM-7822499, and a Research Career Development Award (to D.L.T.).

stable, so that the two will remain associated inside living cells; and 4) The labeling reaction should be mild enough not to abolish the functional activities of the cellular component. Optimally, it is preferable to have a homogeneous preparation of conjugates with the fluorophore attached to well-defined sites, in order to avoid ambiguities involved in the evaluation and interpretation of biochemical as well as spectroscopic data.

Attempts have been made to prepare a fluorescently labeled actin that meets the above criteria. It is known that a sulfhydryl group, located at cys-373, can be blocked without significantly affecting known biochemical activities of actin (17). Therefore, a long-wavelength, highly fluorescent reagent that reacts specifically and irreversibly with sulfhydryl groups should be appropriate for the present purpose. 5-Iodoacetamidofluorescein (5-IAF) has been chosen based on these considerations. In this article, we describe the detailed procedure for preparing 5-IAF-labeled actin (hereafter referred to as 5-AF-actin). The reactive site is characterized by testing the effect of *N*-ethylmaleimide (NEM) pretreatment. The functional activities are assessed based on polymerizability, activation of heavy meromyosin (HMM) Mg^{2+} adenosine triphosphatase (ATPase), formation of paracrystals, and incorporation into a cell-free contractile system. Furthermore, the fluorescence properties are characterized and the application to molecular cytochemistry in vivo is discussed. The incorporation of 5-AF-actin into living ameba and sea urchin eggs has already been reported elsewhere (31–33).

Materials and Methods

Reagents. 5-IAF and lissamine rhodamine B sulfonyl chloride were purchased from Molecular Probes (Plano, TX). NEM, fluorescein isothiocyanate (FITC), dithiothreitol (DTT), and Sephadex G-25 were obtained from Sigma Chemical Co. (St. Louis, MO). ATP was purchased from Boehringer-Mannheim and DEAE-cellulose (DE52) was obtained from Whatman.

Protein preparation and assay. Rabbit striated muscle actin was prepared according to the method of Spudich and Watt (27). Rabbit striated muscle myosin was prepared according to Kieley and Harrington (12). HMM was prepared according to Lowey and Cohen (16). Ovalbumin (Worthington, 2 times crystallized) was labeled using FITC or lissamine rhodamine B sulfonyl chloride as described previously (32, 33). The motile cell-free extract, S3, from *Dictyostelium discoideum* was prepared according to Condeelis and Taylor (3).

Concentrations of labeled proteins were determined by the Lowry procedure. The concentration of unlabeled G-actin and HMM were measured by absorbance at 280 nm, using extinction coefficients of 1.08 and 0.65 $cm^{-1}(mg/ml)^{-1}$, respectively. The molecular weight of actin was assumed to be 42,000 daltons and that of HMM 350,000 daltons.

Extinction coefficient of bound fluorescein. The concentrations of fluorescein bound to actin were determined by absorbance measurements at 495 nm in a buffer (Buffer E) containing 10 mM Tris-HCl, pH 8.0, 0.2 mM $CaCl_2$, 0.5 mM ATP. The extinction coefficient was obtained by the method of Hartig et al. (8). The extinction coefficient of 5-IAF at 495 nm in 7.5 M urea, 10 mM Tris-HCl, pH 8.0, was 6.9×10^4 $cm^{-1}M^{-1}$. The absorbance of 5-AF-actin at 495 nm in Buffer E was 87% that in 7.5 M urea, 10 mM Tris-HCl, pH 8.0. Assuming that 5-IAF and 5-AF-actin had the same extinction coefficient in 7.5 M urea, 10 mM Tris-HCl, the extinction coefficient of 5-AF-actin in Buffer E should be 87% of 6.9×10^4 $cm^{-1}M^{-1}$, or 6.0×10^4 $cm^{-1}M^{-1}$.

NEM treatment of actin. Aliquots of 20 mM NEM stock solution in 3 mM imidazole, pH 7.5, 0.2 mM $CaCl_2$, 0.4 mM ATP, 0.2 mM ascorbic acid were added to 4.0 mg/ml solutions of G-actin in the same buffer. The final concentration of NEM was 0.75 mM. The mixture was put under N_2 atmosphere and stirred at room temperature for 1 hr. The reaction was terminated by adding 2-mercaptoethanol to 1 mM. Quenched NEM was subsequently removed by dialysis.

Fluorescence measurements. Fluorescence intensities and spectra were measured using a Fluorolog spectrofluorometer (Spex Industries, Metuchen, NJ) equipped with an XBO 150 xenon lamp. The intensity fluctuations of the xenon lamp and the variations in the efficiency of excitation monochromator were corrected using a rhodamine B quantum counter in the reference detector. To record excitation spectra, the emission monochromator was fixed at 545 nm with 10 nm bandpass and the excitation monochromator scanned from 400 to 535 nm with 1 nm bandpass. To record emission spectra, the excitation monochromator was fixed at 465 nm with 10 nm bandpass and the emission monochromator scanned from 480 to 600 nm with 1 nm bandpass. To measure peak fluorescence intensities, the excitation and emission monochromators were fixed at 500 and 522 nm, respectively, with 8 nm bandpass for both monochromators. A quartz square microcuvette of 4 mm pathlength was used for all measurements.

The concentration of 5-AF-actin in all samples were 0.01 mg/ml, which was below the critical concentration. A buffer containing 2 mM piperazine-*N*,*N*′-bis (2-ethane sulfonic acid) (PIPES), 2 mM $MgCl_2$ and 0.5 mM DTT (Buffer M) was used for all samples. Samples of G-actin were prepared by direct dilution of monomeric 5-AF-actin into Buffer M immediately before measurements. To prepare polymerized 5-AF-actin, 0.25 mg/ml monomeric 5-AF-actin was first copolymerized with 2 mg/ml unlabeled actin. The copolymers were subsequently diluted 25-fold into 0.5 mg/ml solutions of unlabeled actin in Buffer M. For acto-HMM, F-actin copolymers as described above were diluted 25-fold into solutions of 1.7 mg/ml HMM in Buffer M. These procedures ensured that 1) the inner filter effect was negligible, 2) the G-state was stabilized by subcritical concentrations, 3) the F-state was stabilized by copolymerization with unlabeled actin and dilution with excess unlabeled F-actin, so that the total actin concentrations were well above the critical concentration, and 4) all samples were under identical ionic conditions, so that effects of ionic environment could be ruled out.

Preparation of paracrystals. Mg^{2+} paracrystals were prepared by adding $MgCl_2$ to monomeric 5-AF-actin to a final concentration of 25 mM. Ni^{2+} paracrystals were prepared by adding $NiCl_2$ to monomeric 5-AF-actin to a final concentration of 4 mM. DTT was removed from the solution, since it reacted with Ni^{2+} ions. Ni^{2+} paracrystals from the same test tube were used for both fluorescence microscopic and electron microscopic observations.

Observation and recording of fluorescent images. Fluorescent images were observed with a Zeiss Photomicroscope III equipped with an epi-illumination condensor, using either 25× Neofluar objectives (N.A. 0.60) or 100× oil immersion objectives (N.A. 1.25). A 60 W quartz-halogen lamp was used as the light source. The images were recorded with an RCA TC 1030/H TV image intensifier coupled to an NEC video tape recorder and an RCA TV monitor.

Selected images on the video tapes were photographed from the

TV screen with Kodak Tri-X film ASA 400 at 1/8 sec exposures and developed in D-76 developer for 10 min at 22°C.

Miscellaneous procedures. For viscosity measurements, G-actin was polymerized by adding KCl to 100 mM and $MgCl_2$ to 1.5 mM. After an 8 hr incubation at 25°C, the viscosity was measured using a Cannon-Manning Semi-microviscometer Size 150. The buffer flow time was 29 sec at 25°C. The relationship between specific viscosity and actin concentration is analyzed by linear regression. The reduced viscosity is calculated from the slope of the line; the critical concentration is determined from the *x*-axis intercept.

Actin-activated HMM Mg^{2+} ATPase was measured in a buffer of 15 mM Tris-HCl, pH 7.5, at 24°C, 2 mM $MgCl_2$, 0.4 mM DTT, 2 mM ATP. After incubation for 15 min at 24°C, the concentration of Pi was determined by the method of Pollard and Korn (23). Less than 50% ATP was hydrolyzed during the assay period. The ATPase activity due to HMM alone was substracted from all values.

The Ni^{2+} paracrystals were negatively stained with 2% uranyl acetate and observed with a Philips 301 electron microscope operated at 80 kV.

Results

Preparation of 5-AF-actin

All steps involving fluorescein were carried out under minimum illumination. Specifics of the procedure were as follows.

Step 1: Reaction. A fine slurry of 10 mg 5-IAF in 300 μl acetone was added dropwise to 3 ml of a buffer containing 100 mM boric acid, 100 mM KCl, 4 mM $MgCl_2$, pH 8.5. The dissolved dye solution was mixed with 3 ml of 5 mM Tris-HCl, pH 8.0, 0.2 mM $CaCl_2$, 100 mM KCl, 1 mM ATP, 0.4 mM ascorbic acid, containing 5 mg/ml F-actin. The molar ratio of dye to protein during reaction was 55 to 1. The reaction was carried out for 2 hr at room temperature under N_2 atmosphere, and terminated by adding excess 2-mercaptoethanol. F-actin was then pelleted by centrifugation at 100,000 × *g* for 2 hr.

Step 2: Depolymerization and desalting. The F-actin pellet was resuspended in 2 ml of 5 mM Tris-HCl, pH 8.0, 0.2 mM $CaCl_2$, 1 mM ATP, 1 mM DTT, and depolymerized by adding dropwise, 1 ml of 1.8 M KI, 3 mM $CaCl_2$, 15 mM ATP, pH 7. After stirring for 30 min at 0°C, the depolymerized actin was clarified and loaded onto a 0.5 cm × 50 cm Sephadex G-25 gel filtration column equilibrated with 10 mM Tris-HCl, pH 7.5, 0.1 mM $CaCl_2$, 0.5 mM ATP, 0.5 mM DTT (Buffer B) at 4°C. Fluorescent fractions in the void volume were collected. Following desalting, the molar ratio of bound fluorescein to actin was 0.4–0.5.

Step 3: DEAE-cellulose ion exchange chromatography and second cycle of polymerization–depolymerization. Since the fluorescein group carries net negative charges at neutral pH (20), labeled actin could be separated from unlabeled actin by ion exchange chromatography. The DEAE-cellulose ion exchange chromatography was carried out essentially as described by Gordon et al. (6). A 0.5 cm × 12 cm DE-52 column was saturated with ATP and preequilibrated with Buffer B containing 0.1 M KCl at 4°C. Two to three milliliters of Buffer B were added to the column immediately before and after the desalted fractions were loaded, in order to minimize actin polymerization during loading. Elution was accomplished with a linear gradient of KCl from 0.1 to 0.4 M in Buffer B. The presence of protein and fluorescein in eluted fractions was monitored by their absorbance at 290 and 495 nm, respectively (Figure 1). Two major absorption peaks at 290 nm were detected, corresponding to 0.20 and 0.27 M KCl, respectively. Fractions of both peaks showed increases in viscosity upon warming, but only the second peak absorbed light at 495 nm. Therefore, the first peak was identified as unlabeled actin and the second peak as 5-IAF-labeled actin.

Fractions 31–40 were pooled and warmed to room temperature after the addition of 5 mM $MgCl_2$. Polymerized actin was subsequently collected by centrifugation at 100,000 × *g* for 2 hr. The pellet was resuspended in 0.5–1.0 ml Buffer A at

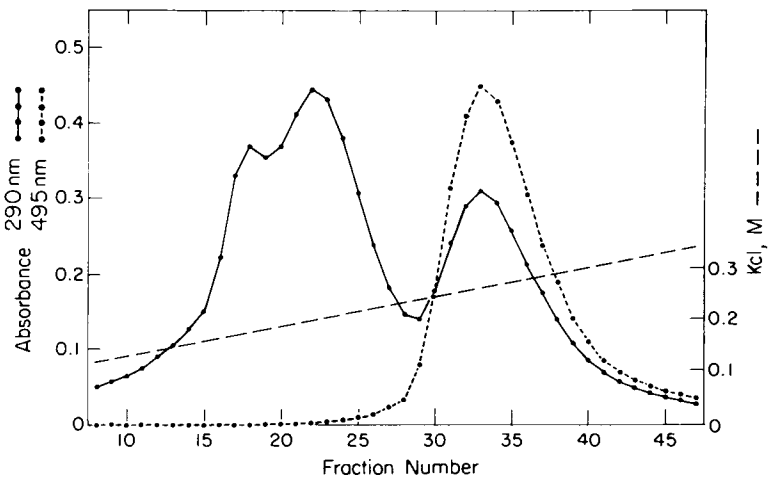

Figure 1. DEAE-cellulose ion exchange chromatography of actin reacted with 5-IAF. The column is eluted with a gradient of KCl (– – –). Absorbances at 290 nm (——) and 495 nm (– · – ·) are measured to follow the elution of protein and fluorescein, respectively. The volume of each fraction is 1 ml.

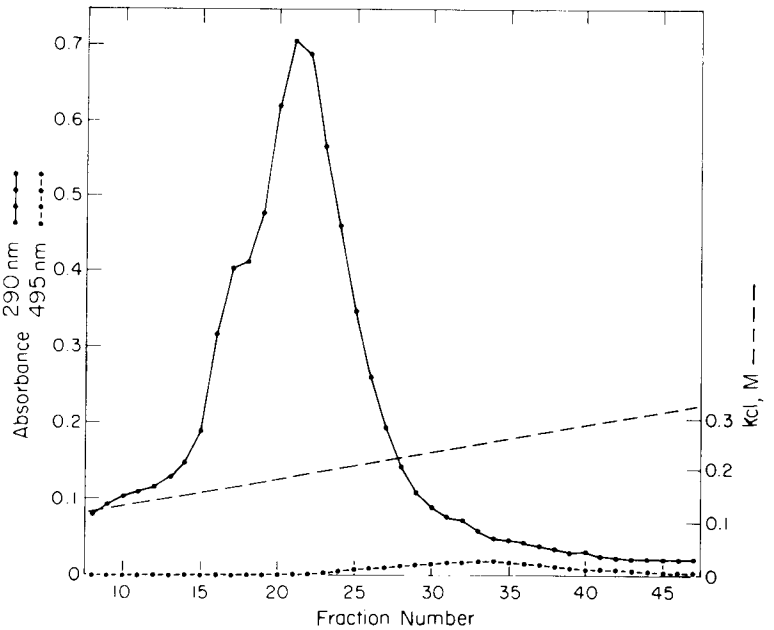

Figure 2. DEAE-cellulose ion exchange chromatography of actin treated with NEM prior to 5-IAF labeling. The total amount of actin is the same as that in Figure 1. Therefore, the peak heights can be directly compared.

4°C (2 mM Tris-HCl, pH 8.0, 0.2 mM $CaCl_2$, 0.2 mM ATP, 0.5 mM DTT, 0.02% NaN_3) and dialyzed for 3 days to depolymerize the 5-AF-actin. The yield of 5-AF-actin was about 20–25% with a fluorescein/actin molar ratio of 0.7–0.9.

Bond Stability and Site of Reaction

To test for the presence of unbound fluorescein and the stability of the association between fluorescein and actin, a solution of 5-AF-actin was made in 1% sodium dodecyl sulfate (SDS) and 1 mM DTT. Following heating to 100°C for 3 min the solution was passed through a Sephadex G-25 column preequilibrated with 10 mM Tris-HCl, pH 8.0, 1 mM DTT, 1% SDS. A single fluorescent peak was detected in the void volume. This result suggested that 1) no unbound fluorescein was present, and 2) the association between fluorescein and actin was covalent and irreversible.

To locate the site of reaction, actin was pretreated with NEM before labeling. A comparison of the elution profile of ion exchange chromatography (Figures 1, 2) indicated that after NEM treatment, the peak of 5-AF-actin decreased by more than 95%, while the peak of unlabeled actin increased correspondingly. This result suggested that 5-IAF reacted predominantly with the same site as NEM, previously determined to be cys-373 (5).

Functional Properties of 5-AF-Actin

The effect of 5-IAF labeling on the biochemical properties of actin was assessed by functional assays in vitro. The reduced viscosity of polymerized 5-AF-actin was 7.2 dl/g under the specified condition, which was 94% that of unlabeled actin (7.7 dl/g). The critical concentration of 5-AF-actin was indistinguishable from that of unlabeled actin (about 0.04 mg/ml under the specified condition, Figure 3). These values fell within the range of values reported previously (7), and suggested that 5-AF-actin maintained normal polymerizability.

5-AF-actin activated the HMM Mg^{2+} ATPase to the same extent as does unlabeled actin (Figure 4). Up to 200-fold activation was observed under the assay condition. The specific activities for both 5-AF-actin and unlabeled actin were ~ 3 μM Pi/μM HMM · μM actin · sec.

Native actin aggregates into paracrystals in the presence of 25–50 mM Mg^{2+} ions (28). The ability of 5-AF-actin to form paracrystals was tested using fluorescence microscopy. Large fluorescent paracrystals (up to 40 μm in length) against a very low background were readily detectable upon adding 25 mM $MgCl_2$ (Figure 5), indicating that essentially all of the 5-AF-actin was incorporated into the paracrystalline structure. The much smaller Ni^{2+} paracrystals (about 3–5 μm in length)

Figure 3. Viscosity assays of 5-AF-actin (○) and unlabeled actin (●). Both are polymerized for 8 hr (25°C) before measuring viscosities in a Cannon-Manning 150 Viscometer. Critical concentrations are indicated by the intercepts on the x-axis.

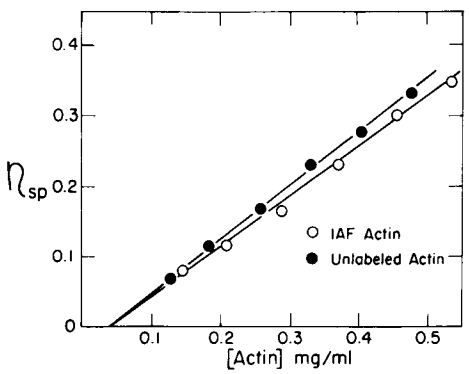

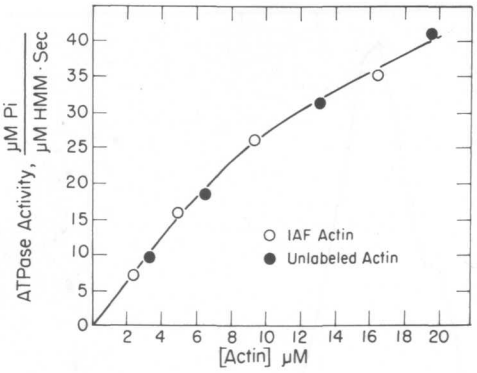

Figure 4. Activation of HMM Mg^{2+} ATPase as a function of 5-AF-actin concentration (○) or unlabeled actin concentration (●). The concentration of HMM varies from 8 to 40 μg/ml, in order to attain about the same rate of ATP hydrolysis (~ 0.06 mM Pi/min). The ATPase activity due to HMM alone (~ 0.2 μM Pi/μM · sec) has been substracted from all values. The conditions for the assay are described under Materials and Methods.

could also be detected (Figure 6A). Electron microscopy of negatively stained Ni^{2+} paracrystals indicated that each paracrystal contained up to 20 actin filaments (Figure 6B), similar to what has been reported for unlabeled actin (28). Samples of F-actin had the appearance of a barely detectable dense meshwork in the fluorescence microscope. However, the signal is too weak to be recorded by the present methods.

Figure 5. Mg^{2+} paracrystals of 5-AF-actin as detected by a fluorescence microscope coupled to a TV image intensifier. Bar = 5 μm.

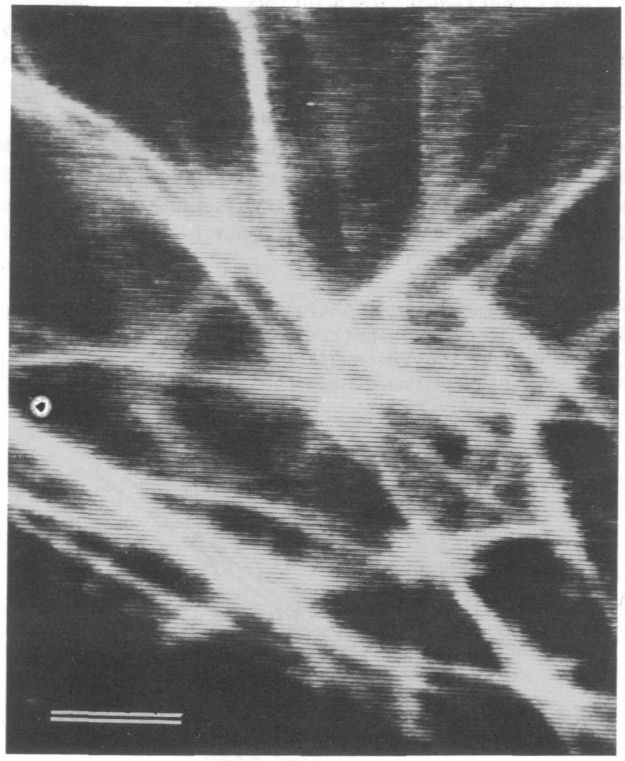

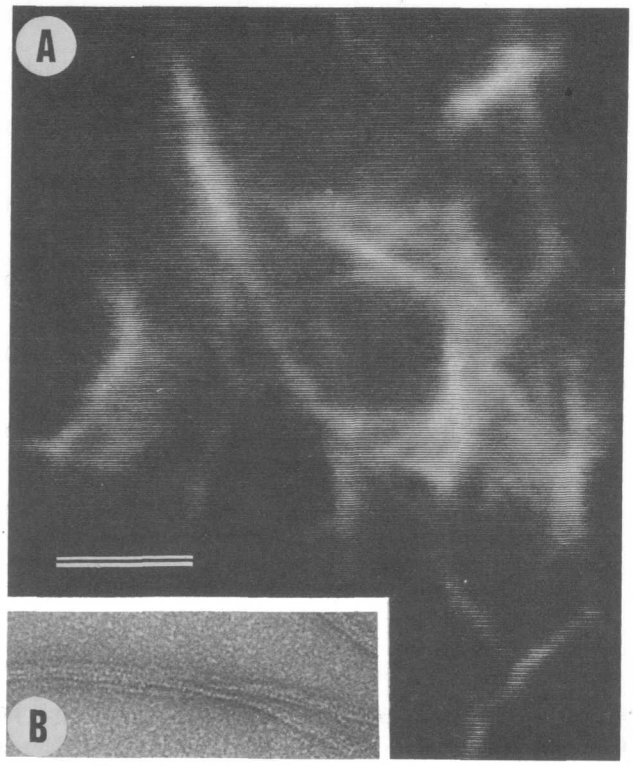

Figure 6. Ni^{2+} paracrystals of 5-AF-actin. (A) As detected by a fluorescence microscope coupled to a TV image intensifier. Bar = 5 μm. (B) Electron microscopy of negatively stained Ni^{2+} paracrystals.

5-AF-actin was further tested to see if it could be incorporated into a cell-free extract from *D. discoideum,* which exhibited Ca^{2+} and pH sensitive contraction with concomitant formation of highly birefringent actin fibrils (3). A mixture of 5-AF-actin and lissamine rhodamine B ovalbumin was added to the extract in order to follow the distribution of the two fluorescent components simultanelusly. The fluorescence of both 5-AF-actin and lissamine rhodamine B ovalbumin remained uniform during the sol-gel transition. However, when solation–contraction of the gel was induced by raising the pH or free Ca^{2+} concentration, fluorescent fibrils containing 5-AF-actin were observed (Figure 7A). In contrast, the lissamine rhodamine B fluorescence remained uniform (Figure 7B). The final contracted pellet consisted of a dense meshwork of small fibrils (Figure 7C). These observations were independent of 5-AF-actin concentrations in the range of 0.15 mg/ml to 0.05 mg/ml (which is close to the critical concentration), suggesting that the incorporation of 5-AF-actin into fibrils was not due to the entrapment of preexisting 5-AF-actin filaments by the contracting gel.

Fluorescence Properties of 5-AF-actin

The fluorescence spectra and peak fluorescence intensities of 5-AF-actin were studied in the monomeric, polymeric, and

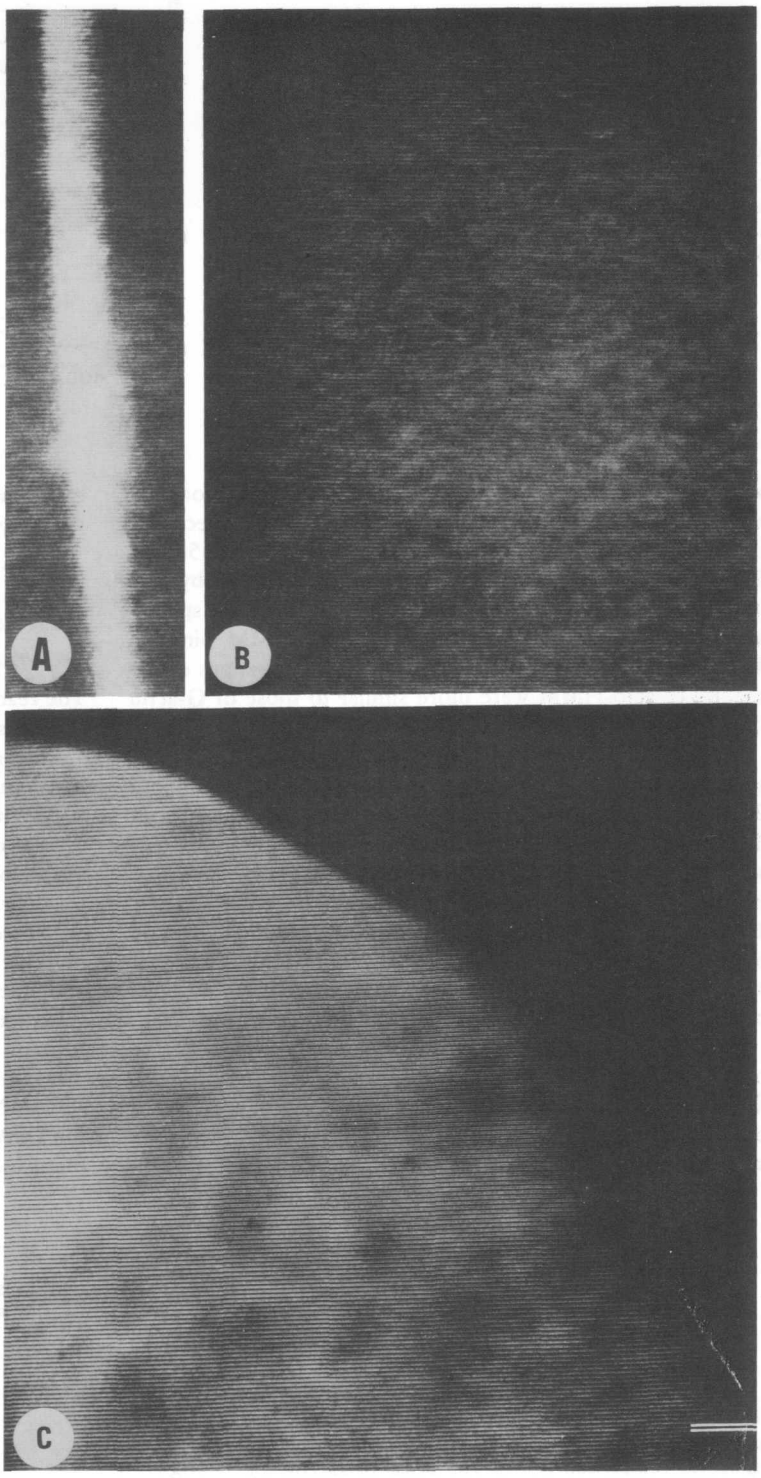

Figure 7. *D. Discoideum* cell-free extract under the fluorescence microscope. 5-AF-actin and lissamine rhodamine B ovalbumin are added to the cell-free extract S3 to 0.1 mg/ml and 0.2 mg/ml, respectively. Contractions are initiated by raising the free Ca^{2+} concentration to $\sim 8 \times 10^{-7}$ M. The contracting bundles are distinctly fluorescent at the 5-AF-actin wavelength (A), while the fluorescence of lissamine rhodamine B ovalbumin remains uniformly distributed (B). A knot of fibrils containing 5-AF-actin is obtained upon completion of contraction (C). Bar = μm.

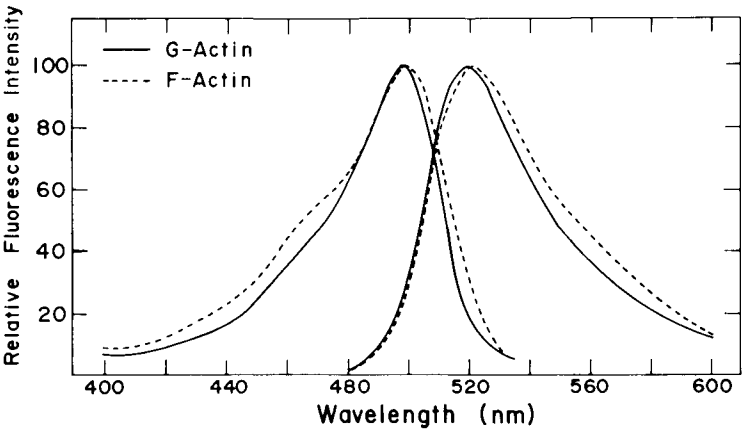

Figure 8. Fluorescence spectra of monomeric (——) and polymerized (– – –) 5-AF-actin. The spectra are normalized to the same peak height. The peaks of spectra for G-actin are located at 498 and 519 nm; and for F-actin at 499 and 521 nm.

acto-HMM states. In the monomeric state, excitation and emission spectra had peaks at 498 and 519 nm, respectively (Figure 8). Small shoulders were observed at 470 and 550 nm. Upon polymerization, both peaks shifted to the red by 1–2 nm and the shoulders became more prominent. The spectra underwent further 3 nm red shifts upon HMM binding. Interestingly, the shoulders diminished and the shapes of the spectra of acto-HMM were more similar to those of G-actin (Figure 9).

The peak fluorescence intensities were also affected by the state of actin. At pH 7.0, F-actin had a peak intensity about 20% lower than that of G-actin, while acto-HMM was about 40% more fluorescent than G-actin (Figure 10). The intensities were highly pH dependent because of the acid–base equilibrium of the fluorescein group (20). As shown in Figure 10, G-actin was slightly more pH sensitive than either F-actin or acto-HMM. Variations in free Ca^{2+} concentrations or ionic strength were found to cause negligible changes in the fluorescence intensity of F-actin.

Control experiments were carried out using FITC-labeled ovalbumin. No changes in fluorescence spectra or peak fluorescence intensities were observed when FITC-labeled ovalbumin was mixed with unlabeled G-actin, F-actin, or acto-HMM, indicating that the changes in fluorescence properties were not caused by changes in light scattering or viscosity.

Discussion

Preparation and Characterization of 5-AF-Actin

The reactivity of 5-IAF is relatively low in aqueous solutions. Previous applications of this reagent have used as much as 1,000-fold molar excess during the reaction to achieve stoichiometric labeling (8). In order to attain high reaction specificity, the molar excess in the present study has been limited to 55-fold. Under this condition, only 40 to 50% of the actin reacts with 5-IAF. Therefore, a procedure involving polymerization cycles, gel filtration, and ion exchange chromatography is employed to obtain a homogeneous fraction that is covalently labeled at a molar ratio close to 1.

Under our reaction condition, 5-IAF should react specifically with sulfhydryl groups (21). Any trace of nonspecific reaction products with lysine residues should be removed by the DEAE-cellulose ion exchange chromatography. The results of NEM treatment suggest that the pooled fractions from the DEAE-cellulose column contain a relatively homogeneous population of labeled actin, with the fluorescein group bound

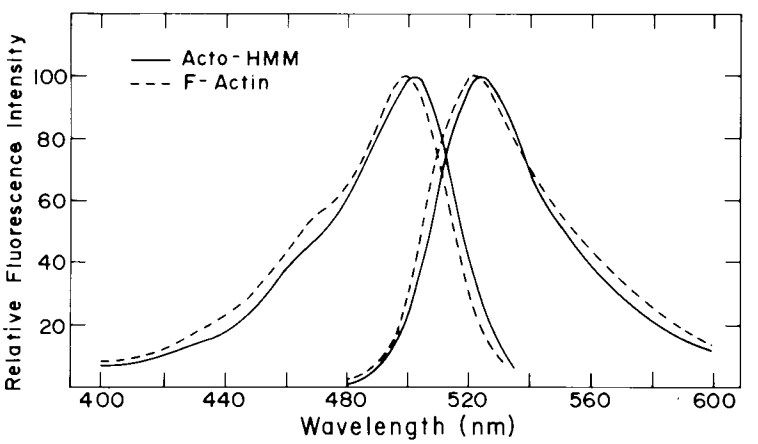

Figure 9. Fluorescence spectra of 5-AF-actin in the acto-HMM (——) state. The spectra of F-actin are redrawn for comparison (– – –). The peaks of spectra for acto-HMM are located at 502 and 524 nm.

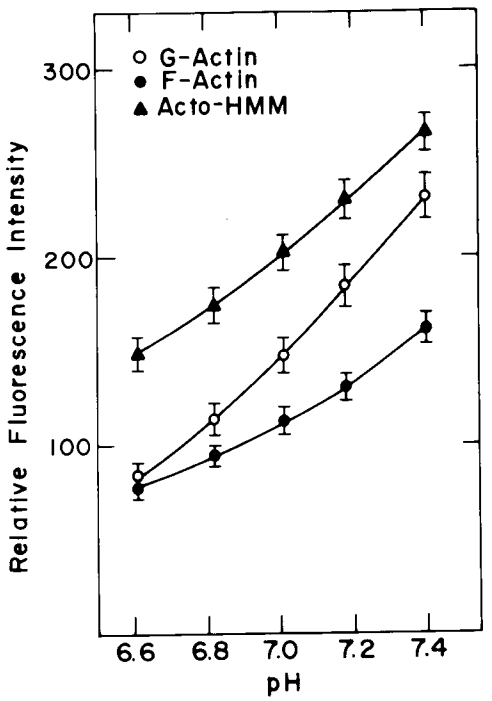

Figure 10. Relative peak fluorescence intensities as a function of pH and states of actin. 5-AF-actin is excited at 500 nm and the intensities of light emitted at 522 nm are measured.

predominantly to the same site as that for NEM, namely cys-373 (5). This result is consistent with previous reports using different iodoacetamido reagents (5, 17, 25).

The results of the biochemical assays indicate that 5-AF-actin is functionally very similar to unlabeled actin. Specifically, these results suggest that reaction with 5-IAF does not block the active sites for polymerization, myosin binding, or paracrystal formation. In addition, as 5-AF-actin is stable in vitro, the high-affinity binding sites for divalent cations and nucleotides are not likely to be affected (22). These observations are consistent with previous studies on the modification of cys-373 (4, 17).

In view of the fact that cys-373 is highly conserved through evolution, it is possible that some as yet uncharacterized functions are affected. Many more experiments must be carried out before a complete assessment can be made. Nevertheless, the present results suggest that 5-AF-actin is a good analog for studying at least some biological functions of actin.

Fluorescence Properties of 5-AF-Actin

The microenvironment of actin cys-373 has been investigated extensively using fluorescence spectroscopy. The polymerization of actin is accompanied by a decrease in the accessibility of cys-373 to the aqueous milieu (29); the microenvironment undergoes a slight change, as reflected by changes in fluorescence spectra (15, 25, 26). An increase in energy transfer is observed from tryptophan residues to the probe, possibly due to changes in local conformation (26). The binding of myosin heads to F-actin is marked by a decrease in microenvironmental polarity and a further increase in the energy transfer from tryptophan residues (26). The probe becomes appreciably immobilized as indicated by polarization measurements (11).

Compared to other probes, fluorescein has several special characteristics. 1) Both absorption and fluorescence are highly pH-dependent, due to the acid–base equilibria (20). The monoanionic form is gradually replaced by the dianionic form when pH is increased from 6.0 to 8.0. Accompanying this transition are increases in extinction coefficient and quantum yield, and decreases in the shoulders of both absorption and emission spectra. 2) Both absorption and fluorescence are sensitive to solvent properties, presumably hydrogen-bonding ability (19). For the dianionic form, it is demonstrated that increasing hydrogen-bonding ability would decrease the extinction coefficient and blue-shift the peak absorption and fluorescence wavelengths. 3) The fluorescence is sensitive to a number of quenchers (34). While the effect of molecular oxygen is found to be negligible, tryptophan is highly effective (34). The fluorescence of protein-bound fluorescein is therefore sensitive to the presence of neighboring tryptophan residues. This effect has been used to explain the quenching of fluorescence when fluorescein is associated with anti-fluorescein antibodies (34).

The changes in fluorescence properties of 5-AF-actin in different states cannot be explained by any single factor mentioned above, and are most likely caused by a combination of changes in several microenvironmental factors. For example, the changes in the shoulders of the spectra could be caused by changes in the pK_a value of fluorescein or in local proton activity. On the other hand, the red shifts upon polymerization and HMM binding could be caused by decreases in hydrogen-bonding ability of the microenvironment. In addition, the proximity of tryptophan residues to cys-373 might also affect the intensities of fluorescence.

Applications

The visibility of Ni^{2+} paracrystals indicates that 5-AF-actin bundles containing as few as 20 filaments or about 7,000 fluorescein groups per μm can be readily detected. If 5-AF-actin is incorporated into a motile system to a concentration 10% that of endogenous actin, fibrils of 200 actin filaments should be detectable. This high sensitivity not only allows us to observe actin-containing fibrils in the cell-free extract (Figure 7C), but also makes it possible to follow the formation and transformation of small actin-containing structures such as paracrystals and cytoplasmic fibrils in real time (32).

The sensitivity of fluorescence properties makes 5-AF-actin a valuable tool for following the conformational changes of actin. When pH is known, intensity changes or spectral shifts could provide information about the transformation of actin states (Taylor, unpublished data). Furthermore, the nature of the absorption and emission spectra makes fluorescein an excellent probe for resonance energy transfer studies. By placing an energy donor or acceptor on an actin-binding component, molecular interactions such as actin polymeriza-

tion, actin–myosin interaction, and interactions with other proteins or ligands could be investigated.

Finally, the present results suggest that 5-AF-actin fulfills the requirements for in vivo molecular cytochemistry. The absorption and fluorescence properties are compatible with living cells; the association between the fluorescein group and actin is stable; and the major biochemical activities are indistinguishable from those of unlabeled actin. Future applications of 5-AF-actin in vivo could elucidate: 1) The formation and transformation of actin-containing structures, using fluorescence microscopy coupled to image intensification techniques; 2) The state of actin assembly, using microspectrofluorometry; and 3) The mobility of actin, as measured by the photobleaching recovery technique. Photobleaching could also be used to disrupt actin-containing structures in specific regions.

Acknowledgments

The authors would like to thank L. Meszoly, J. Miller, and S. Hellewell for technical assistance. They would also like to thank Drs. E. Haas and E. Simons for helpful discussions, and J. Heiple and V. Fowler for critically reading the manuscript.

Literature Cited

1. Carlsson L, Nyström LE, Lindberg U, Kannan KK, Cid-Dresdner H, Lövgren S, Jornvall H: Crystallization of a non-muscle actin. J Mol Biol 105:353, 1976
2. Cheung HC, Cooke R, Smith L: The G-actin F-actin transformation as studied by the fluorescence of bound dansyl cystine. Arch Biochem Biophys 142:333, 1971
3. Condeelis JS, Taylor DL: The contractile basis of amoeboid movement V. The control of gelation, solation, and contraction in extracts from Dictyostelium discoideum. J Cell Biol 74:901, 1977
4. Drabikowski W, Gergely J: The role of sulfhydryl groups in the polymerization and adenosine triphosphate binding of G-actin. J Biol Chem 238:640, 1963
5. Elzinga M, Collins JH: The primary structure of actin from rabbit skeletal muscle. J Biol Chem 250:5897, 1975
6. Gordon DJ, Eisenberg E, Korn ED: Characterization of cytoplasmic actin isolated from Acanthamoeba castellanii by a new method. J Biol Chem 251:4778, 1976
7. Gordon DJ, Yang Y-Z, Korn ED: Polymerization of Acanthamoeba actin. Kinetics, thermodynamics, and copolymerization with muscle actin. J Biol Chem 251:7474, 1976
8. Hartig PR, Bertrand NJ, Sauer K: 5-iodoacetamidofluorescein-labeled chloroplast coupling factor I: conformational dynamics and labeling-site characterization. Biochemistry 16:4275, 1977
9. Hatano S, Owaribe K: Some properties of Physarum actinin, a regulatory protein of actin polymerization. Biochim Biophys Acta 579:200, 1979
10. Ikkai T, Wahl P, Auchet J-C: Anisotropy decay of labelled actin. Eur J Biochem 93:397, 1979
11. Kawasaki Y, Mihashi K, Tanaka H, Ohnuma H: Fluorescence study of N-(3-pyrene) maleimide conjugated to rabbit skeletal F-actin and plasmodium actin polymers. Biochim Biophys Acta 446:166, 1976
12. Kielly WW, Harrington WF: A model for the myosin molecule. Biochim Biophys Acta 41:401, 1960
13. Korn ED: Biochemistry of actomyosin-dependent cell motility (a review). Proc Natl Acad Sci USA 75:588, 1978
14. Lazarides E, Lindberg U: Actin is the naturally occurring inhibitor of deoxyribonuclease I. Proc Natl Acad Sci USA 71:4742, 1974
15. Lin T-I: Fluorimetric studies of actin labeled with dansyl aziridine. Arch Biochem Biophys 185:285, 1978
16. Lowey S, Cohen C: Studies on the structure of myosin. J Mol Biol 4:293, 1962
17. Lusty CJ, Fasold H: Characterization of sulfhydryl groups of actin. Biochemistry 8:2933, 1969
18. Lux SE: Dissecting the red cell membrane skeleton. Nature 281:426, 1979
19. Martin MM: Hydrogen bond effects on radiationless electronic transitions in xanthene dyes. Chem Phys Lett 35:105, 1975
20. Martin MM, Lindqvist L: The pH dependence of fluorescein fluorescence. J Luminescence 10:381, 1975
21. Means GE, Feeney RE: Chemical Modification of Protein. Holden-Day, San Francisco, 1971
22. Oosawa F, Kasai M: Subunits in Biological Systems, Part A. Edited by SN Timasheff, GD Fasman. Marcel Dekker, New York, 1971 p 261–322
23. Pollard TD, Korn ED: Acanthamoeba myosin I. Isolation from Acanthamoeba castellanii of an enzyme similar to muscle myosin. J Biol Chem 248:4682, 1973
24. Pollard TD, Weihing RR: Actin and myosin and cell movement. Crit Rev Biochem 2:1, 1974
25. Porter M, Weber A: Non-cooperative response of actin-cystin 373 in cooperatively behaving regulated actin filaments. FEBS Lett 105:259, 1979
26. Sekine T, Ohyashiki T, Machida M, Kanaoka Y: Studies on calcium ion-induced conformation changes in the actin-tropomyosin-troponin system by fluorimetry. Biochim Biophys Acta 351:205, 1974
27. Spudich JA, Watt S: The regulation of the rabbit muscle contraction I. Biochemical studies of the interaction of the tropomyosin-troponin complex with actin and the proteolytic fragments of myosin. J Biol Chem 246:4866, 1971
28. Strzelecka-Golaszewska H, Prochniewica E, Drabikowski W: Interactions of actin with divalent cations I. The effect of various cations on the physical state of actin. Eur J Biochem 88:219, 1978
29. Tao T, Cho J: Fluorescence lifetime quenching studies on the accessibilities of actin sulfhydryl sites. Biochemistry 18:2759, 1979
30. Taylor DL, Condeelis JS: Cytoplasmic structure and contractility in amoeboid cells. Int Rev Cytol 56:57, 1979
31. Taylor DL, Wang Y-L: Molecular cytochemistry: incorporation of fluorescently labeled actin into living cells. Proc Natl Acad Sci USA 75:857, 1978
32. Taylor DL, Wang Y-L, Heiple JM: The contractile basis of amoeboid movement. VII. Distribution of fluorescently-labeled actin in living amoeba. J Cell Biol, in the press
33. Wang Y-L, Taylor DL: Distribution of fluorescently labeled actin in living sea urchin eggs during early development. J Cell Biol 82:672, 1979
34. Watt RM, Voss EW Jr: Mechanism of quenching of fluorescence by antifluorescein IgG antibodies. Immunochemistry 14:533, 1977